

Microstructural and Electrochemical Characterization of Friction Stir Welded Duplex Stainless Steels

Marina Magnani^{1,2*}, Maysa Terada¹, Amanda Osteno Lino¹, Vanessa P. Tallo¹,
Eduardo Berton da Fonseca¹, Tiago F. A. Santos^{1,3}, Antonio J. Ramirez¹

¹ Laboratório Nacional de Nanotecnologia (LNNano), CP 6192, Campinas-SP, 13083-970, Brazil

² Now at, Instituto de Química, UNESP, CP 355, Araraquara-SP, 14800-900, Brazil

³ Now at, Centro de Pesquisa e Desenvolvimento em Telecomunicações (CPqD), Rodovia Campinas - Mogi-Mirim, km 118,5, Campinas, 13086-902, SP – Brazil

*E-mail: marina@iq.unesp.br

Received: 8 October 2013 / Accepted: 29 January 2014 / Published: 23 March 2014

Duplex stainless steels exhibit good mechanical properties and corrosion resistance as well as better weldability and lower sensitivity to the weld cracking. The friction stir welding is based on a tool to generate heat and deformation. This process has been studied to applications in oil/gas pipes, aerospace industry and equipments. In this work, the corrosion resistance of two friction stir welded (FSWed) samples (UNS S32205 and lean duplex UNS S32101) was evaluated using electrochemical impedance spectroscopy and the results were fitted to electric equivalent circuits. The electrochemical results indicate the presence of a high stability oxide of both duplex stainless steels not only at the base metal but also at the stir zone of the friction stir welded samples. All Bode phase diagrams presented two peaks associated to the oxide layer formed on the surface of stainless steels and the charge transfer. The corrosion resistance of the UNS S32205 was improved and the lean duplex UNS S32101 was decreased after friction stir welding process (FSW). Nevertheless, the resistance of the UNS S32101 FSWed was still similar or higher than the traditional austenitic stainless steels.

Keywords: FSW, lean duplex UNS S32101, UNS S32205, EIS

1. INTRODUCTION

Duplex stainless steels (DSSs), balanced with ferrite (α) and austenite (γ) phases exhibit good mechanical property and corrosion resistance as well as better weldability and lower sensitivity to the weld cracking [1]. This enables various types of DSSs application such as chemical and petrochemical industries [2-3].

The *ruling class* of DSS is the conventional UNS S32250, developed in the 1970s to compete with the class of austenitic stainless steels AISI 904L. Continuous changes in alloy composition were made to improve the corrosion resistance, formability and weldability. In particular, the addition of nitrogen was used to improve the pitting corrosion resistance and the weldability [4,5]. The duplex stainless steel low alloy (UNS S32101), substitutes nickel by nitrogen and manganese. This composition aims to diminish the dependence of alloying elements with variable prices so as nickel and molybdenum.

However, the fusion welding processes, associated with the melting and solidification, destroys the favorable duplex microstructure of stainless steels, resulting in a microstructure consisting of coarse ferrite grains, and both intergranular and intragranular austenite phases in the weld metal and heat affected zone (HAZ) [6]. These changes of the microstructure can decrease the corrosion resistance in the weld. To avoid this problem, solid-state joining technologies as friction stir welding (FSW) has attracted considerable attention [7].

The friction stir welding technique is based on a tool to generate heat and deformation [3]. The resultant joint presents different areas as the heat affected zone, thermomechanical affected zone and stir zone. The main advantages of this process are the solid state welding, the absence of metal of addition, and the fast cooling, avoiding precipitation. This process has been studied to applications in oil/gas pipes, aerospace industry and equipments.

There are only a few studies in the literature on the corrosion behavior of stainless steels FSWed. Park *et al* evaluate the corrosion properties of an FSWed AISI 304 stainless steel, especially the advancing side of the stir zone and its heat affected zone (HAZ) and they observed a little amount of sensitization in the heat affected zone, but the advancing side of the stir zone was corroded due of the formation of the sigma phase [8]. A pitting corrosion of four different zones of welded austenitic stainless steels (AISI 304 and 316L) using a micro-cell was also studied by Garcia *et al.* with a specific small-scale electrochemical cell. The results showed that the HAZ was the most critical zone for pitting corrosion for both materials due the degree of sensitization [9].

The objective of the present study was to evaluate the corrosion resistance of the stir zone of FSWed samples in comparison with the base metal. In this work, the corrosion resistance of two FSWed DSS samples (S32205 and S32101) was evaluated using electrochemical impedance spectroscopy (EIS) in a 0.1 NaCl solution.

2. EXPERIMENTAL

The experiments were performed at the Brazilian Nanotechnology National Laboratory (LNNano - CNPEM). The investigated materials were UNS2205 and UNS S2101 with the nominal chemical compositions shown in Table 1.

Duplex stainless steel plates of 300 mm (L), 50 mm (W), 12 mm (T) were friction stir welded using a dedicated TTI® machine and an un-tilted polycrystalline cubic boron nitride (PCBN) with 40%-vol. W-Re (25% Re) threaded tool with pin length of 6.4 mm and shoulder diameter of 25 mm. The welds were performed in force control mode with 200 rpm of spindle speed and 100 mm/min of welding speed. The process was performed in the normal direction to the rolling direction in order to

compare to the pipeline arc-welding circular joints, under argon atmosphere. The tool achieved a maximum temperature below 850 °C.

Table 1. Nominal chemical compositions of tested duplex stainless steels (wt %).

| Duplex | C | Cr | Ni | Mn | Mo | N | Fe |
|--------|------|------|-----|-----|-----|-----|-----|
| S32101 | 0.02 | 21.4 | 1.6 | 5.1 | 0.2 | 0.2 | Bal |
| S32205 | 0.02 | 22.5 | 5.4 | 1.8 | 2.8 | 0.2 | Bal |

Samples of 1.0 cm² were prepared before corrosion tests by grinding with silicon carbide paper up to #4000, polishing with diamond paste up to 1 μm, and then washed with isopropanol, dried under hot air stream and then immersed in naturally aerated 0.1 mol L⁻¹ NaCl solution at 25 °C. Microstructural observations were performed by optical microscopy (OM) and scanning electron microscopy (SEM) equipped with an energy-dispersive X-ray spectroscopy (EDS) analysis system – a FEG 650 Quanta FEI. The amount of ferrite was determined in each sample using Electron Backscattering Diffraction.

The electrochemical tests were performed using a three-electrode cell set-up, with a platinum wire and an Ag/AgKCl electrode as counter and reference electrodes respectively.

3. RESULTS AND DISCUSSION

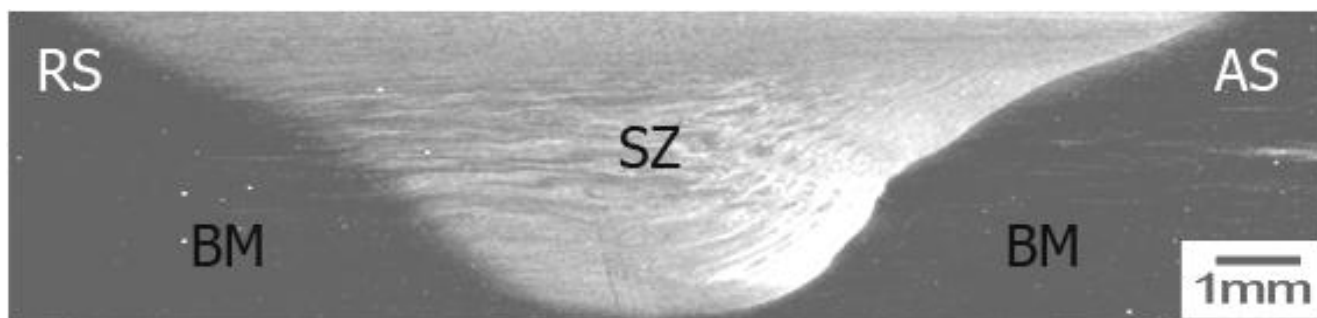


Figure 1. Macrostructure of S32205 sample showing BM (base metal) and the stir zone (SZ).

Figure 1 show a typical macrostructure of the cross section at different regions of FSWed sample. In the cross-section, the left and right sides of the weld center are related to the retreating (RS) and advancing sides (AS) of the rotating tool, respectively. The microstructure of the welded sample can be classified into two distinct regions including the stir zone (SZ) and, the base metal (BM). The heat-affected zone (HAZ) and the thermo-mechanically affected zone (TMAZ) are not clearly observed.

The microstructure of both unaffected materials – UNS S32101 and UNS S32205 (base metal) – is shown in Figure 2. The microstructure consists in white austenite (γ) islands are embedded in a gray matrix of ferrite (α).

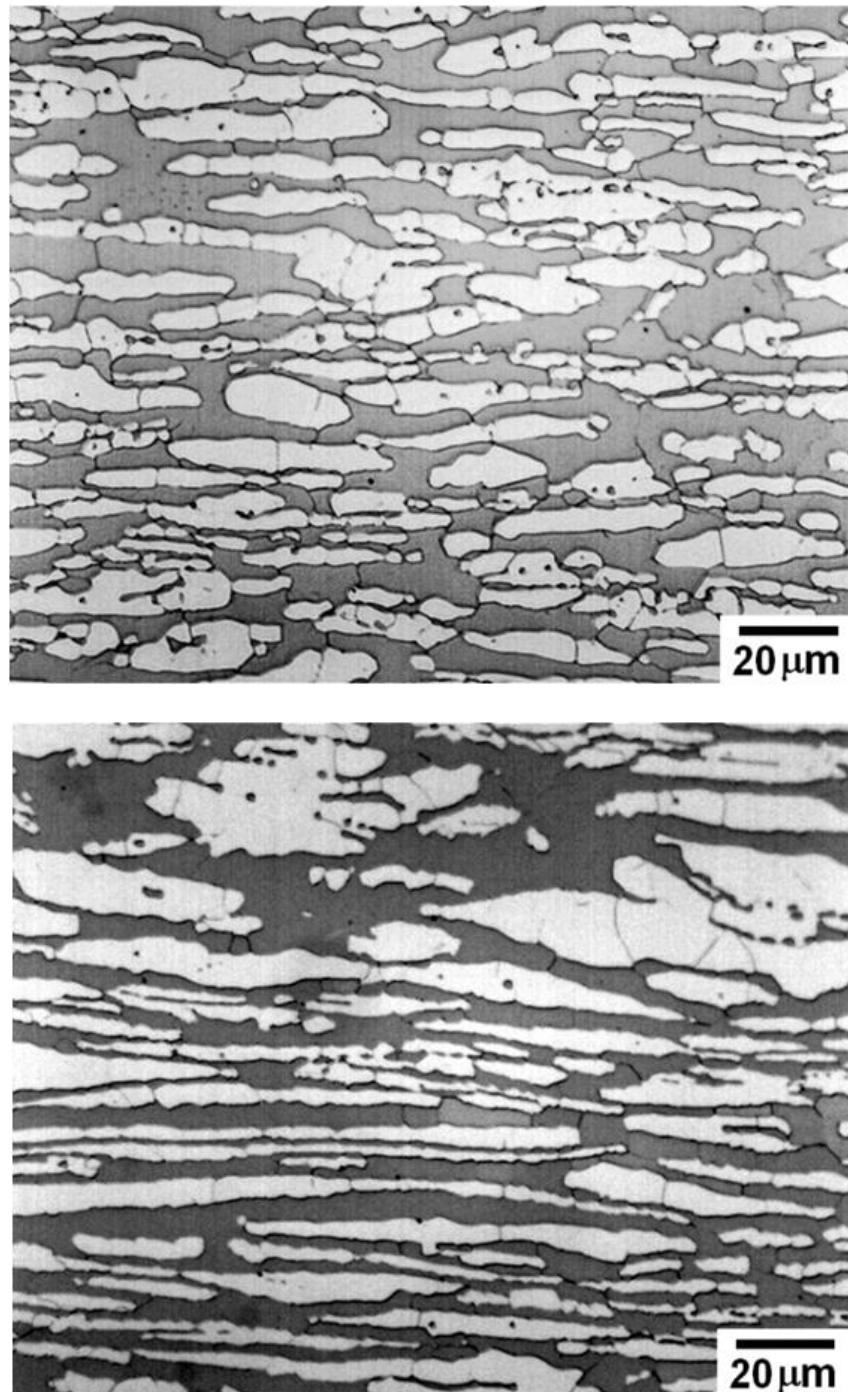


Figure 2. Base metal of UNS (a) S32101 and (b) S32205 DSS [10]. Electrolytic etching: 60% HNO₃ in distilled water. Optical microscopy.

The refinement microstructure in the stir zone (SZ) was distinct from that of the base metal as shown in Figure 3.

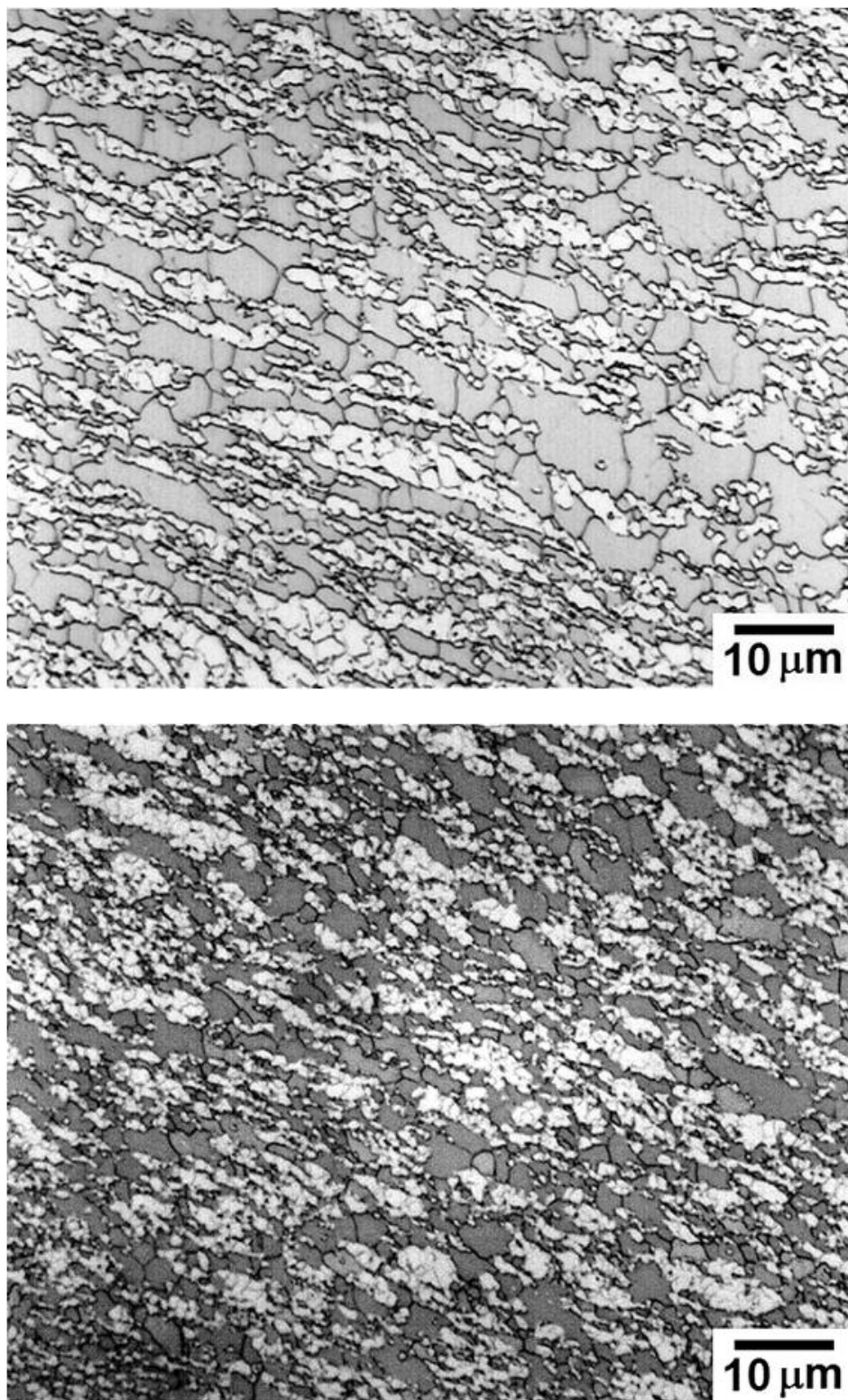


Figure 3. Stir zone of UNS (a) S32101 and (b) S32205 DSS showing the outstanding grain size refinement. Electrolytic etching: 60% HNO₃ in distilled water. Optical microscopy.

The SZ consists of fine equiaxed grains more pronounced in the austenite phase, suggesting that the ferrite has a higher diffusion rate than austenite, producing a recrystallization followed by

grain growth. Besides, the distorted structure caused by the heat effect and mechanical deformation of the material (Figure 3a and 3b) was due to the intense plastic strain in high temperature which the both phases was submitted during FSW, achieving an outstanding grain size refinement. The refinement grain is achieved by continuous and discontinuous dynamic recrystallization in ferrite and austenite, respectively [6,11]. Several authors [10-13] have indicated that the mechanism to increase of mechanical performance is by Hall-Petch relation for duplex and superduplex stainless steels.

Most of phases that use to precipitate in duplex stainless steels during welding decrease the corrosion resistance due to the sensitization of the matrix. However, it was not possible to find deleterious phases as sigma, for example, commonly found in samples welded by other processes. The absence of these phases is due to the rapid cooling of the welding, exceptionally rapid to their nucleation and growth.

The amount of ferrite of both UNS S32101 and UNS S32205 DSS – base metal (BM) and stir zone (SZ) - was measured using Electron Backscattering Diffraction (EBSD), as the high corrosion resistance of duplex stainless steel is due to the balanced ferrite (α) and austenite (γ) phases.

Table 2. Amount of ferrite (%) presented in UNS S32101 and UNS S32205 DSS. Samples of base metal (BM) and stir zone (SZ). EBSD.

| Sample | Ferrite (%) |
|-----------|-------------|
| S32101 BM | 48.8 |
| S32101 SZ | 52.1 |
| S32205 BM | 56.5 |
| S32205 SZ | 46.6 |

Table 2 shows that after the friction stir welding, in contrast with the traditional welding processes, the amount of ferrite in the UNS S32205 SZ decreased from 56.5% to 46.6%. On the other hand, the lean duplex UNS S32101 BM contained 48.8% of ferrite and after welding, this percentage increased to 52.1%. Thus, electrochemical tests were performed in order to evaluate the characteristics of the passive layer formed on the FSWed samples. The measurements were taken after 5, 24, 48, 72, 96 and 120 h after immersion in a naturally aerated 0.1 mol L⁻¹ NaCl solution at 25 °C.

The electrochemical impedance spectroscopy (EIS) Bode-phase angle plots showed two time constants for all samples. High phase angles are seen over a large frequency range, typical of passive materials, likely due to the passive layer on the surface.

The EIS results obtained for the UNS S32205 base metal (BM) are presented in Figure 4. The decrease in phase angles at low frequencies indicates that the passive layer becomes increasingly less protective, being more porous and with increasing amounts of defects. The resistance of the oxide layer decreases from 5 to 24 h and its value maintains stable until 72 h (around 2.40 M Ω .cm²). Despite the measurement taken after 96 h of immersion indicates that the resistance increased (2.83 M Ω .cm²), this could be caused by the products of corrosion deposited on the surface, as after 120 h, the resistance decreased to 2.30 M Ω .cm².

After the welding, the EIS measurements were taken one more time for the UNS S32205 FSWed (SZ) and the results are presented in Figure 5. The Bode Phase diagrams shown two time constants.

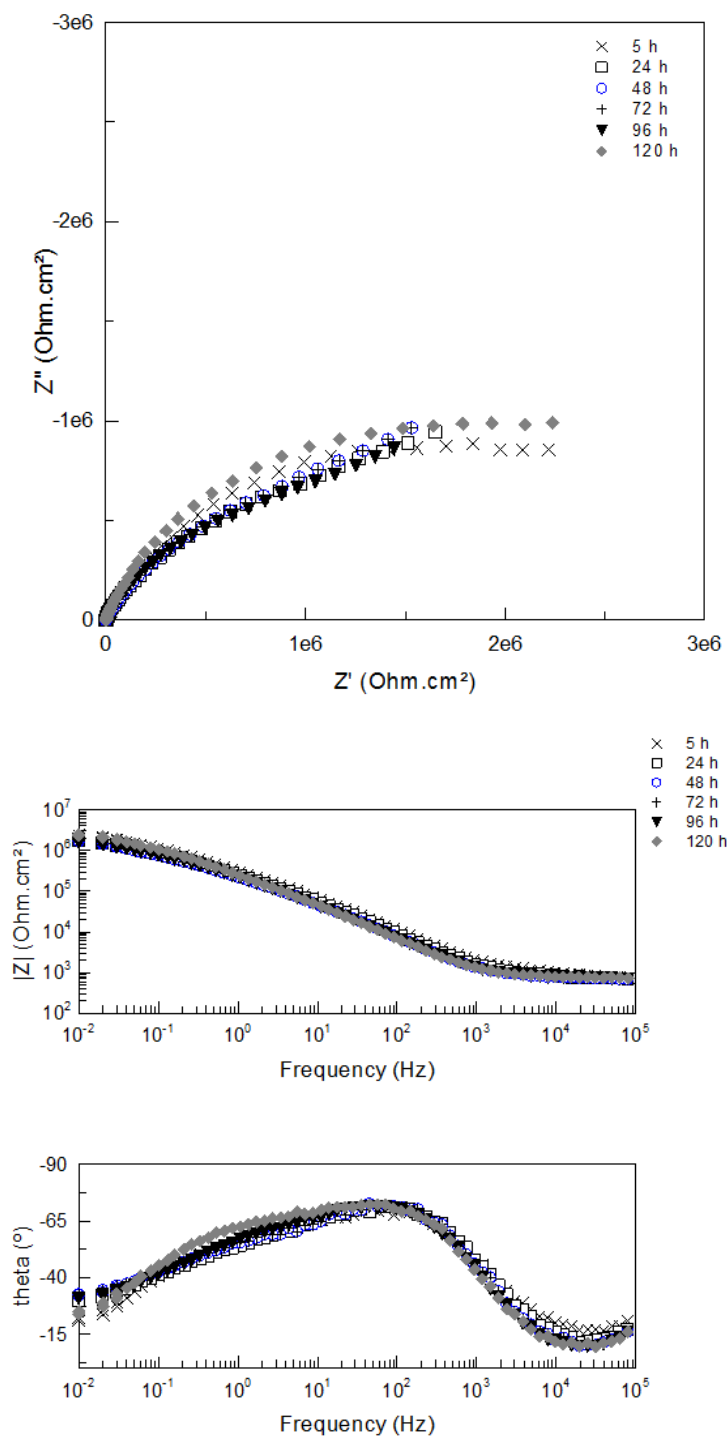


Figure 4. EIS of UNS 32205 duplex stainless steel base metal. A) Nyquist, B) Z Modulus and Bode phase angle diagrams.

The resistance of the oxide layer also decreases from 5 to 24 h. However, afterwards, the resistance increases continuously until 120 h of immersion. As the UNS S32205 BM, this results suggest that the external oxide layer (more porous and with more defects) was removed at the first hours of immersion and then the internal oxide layer became more and more homogeneous and resistant.

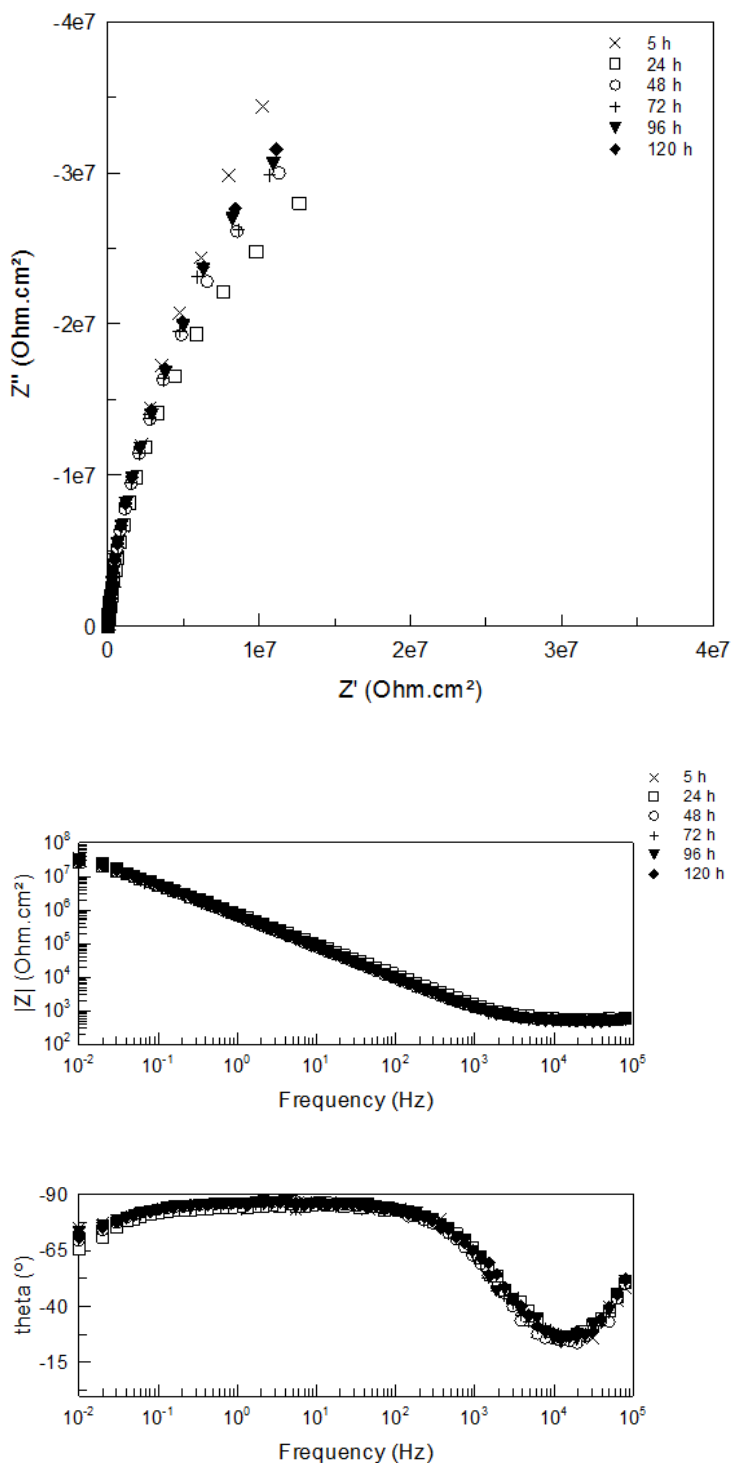


Figure 5. EIS of UNS 32205 duplex stainless steel FSWed. A) Nyquist, B) Z Modulus and Bode phase angle diagrams.

EIS tests indicated that the FSW enhanced the corrosion resistance of the UNS S2205. The resistance of the oxide layer improved in order to 10^2 .

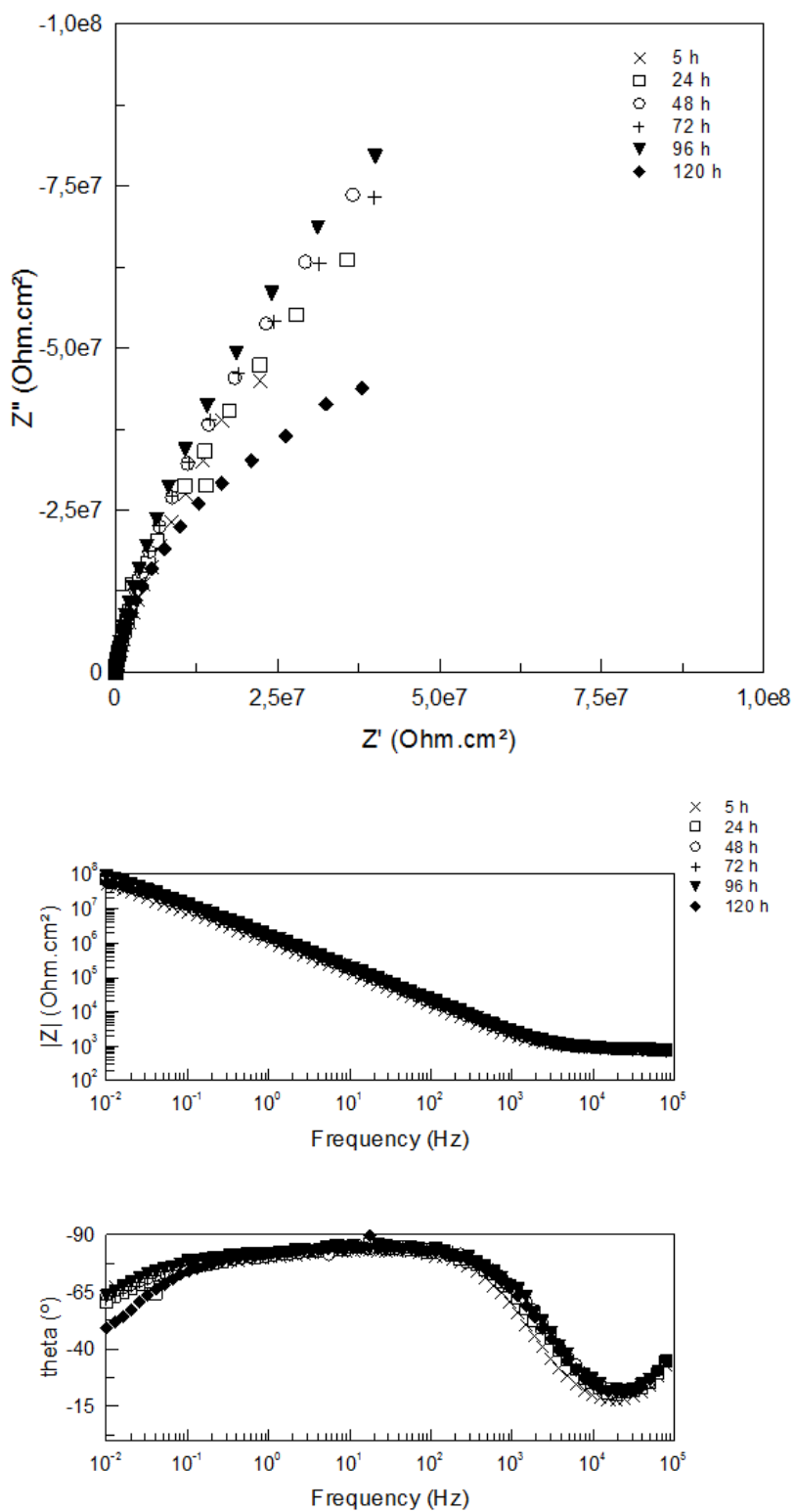


Figure 6. EIS of UNS 32101 lean duplex stainless steel base metal. A) Nyquist, B) Z Modulus and Bode phase angle diagrams.

The EIS tests were also performed for the lean duplex UNS S32101 base metal (BM), presented in Figure 6. On the contrary of the UNS S32205 DSS, the resistance of the oxide layer increases from 5 to 24 h and then decreases until 120 h. However, the resistance of the lean duplex UNS S32101 BM is around $10^8 \Omega.cm^2$ whereas the UNS S32205 BM presented $10^6 \Omega.cm^2$. These results could be related to the amount of ferrite in each sample, as this phase is preferentially corroded in duplex stainless steels.

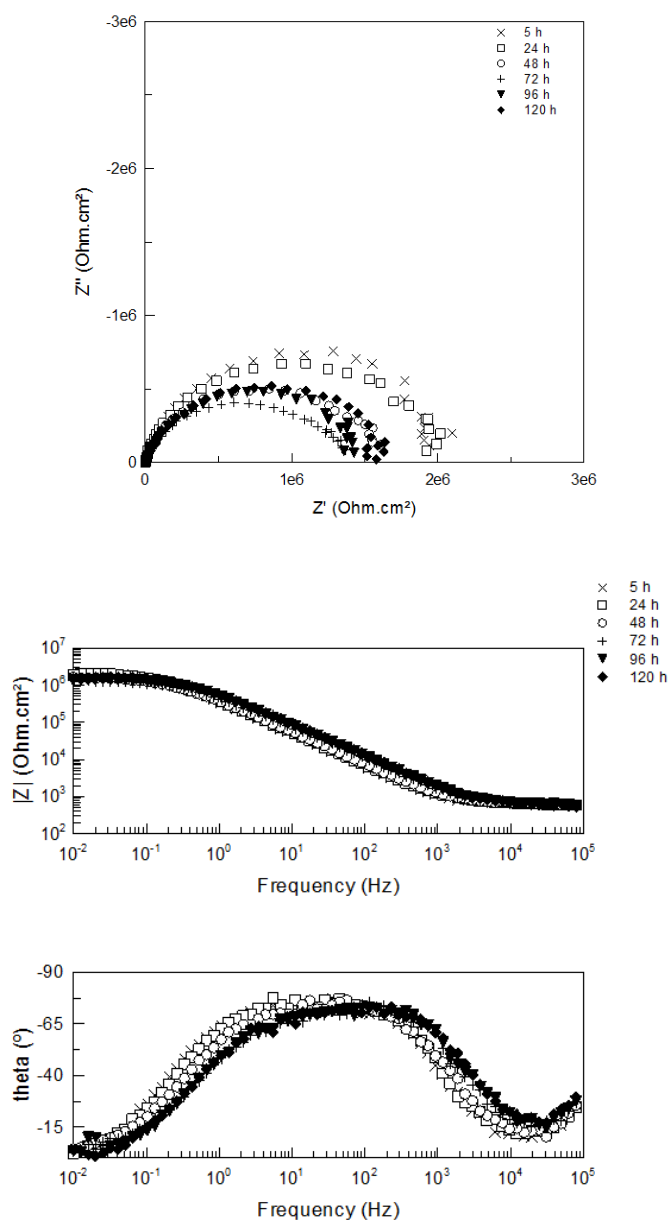


Figure 7. EIS of UNS 32101 lean duplex stainless steel FSWed. A) Nyquist, B) Z Modulus and Bode phase angle diagrams.

After the welding, the EIS measurements were also taken for the lean duplex UNS S32101 FSWed (SZ) and the results are presented in Figure 7. However, the oxide layer formed on the surface of the FSWed samples was more homogeneous and less resistant than the one formed on the base

metal. These results indicate that the FSW decreased the corrosion resistance of the UNS S2101 lean DSS. Nevertheless, the resistance of the oxide layer is in order to $10^6 \Omega \cdot \text{cm}^2$, considered similar or even higher than the traditional austenitic stainless steels.

4. CONCLUSIONS

The Friction Stir Welded (FSWed) samples did not present deleterious phases due to the rapid cooling of the samples. The microstructures of the stir zone showed the presence of fine equiaxed grains, more pronounced in the austenite phase. This suggests that the ferrite has a higher diffusion rate than austenite, producing a recrystallization followed by grain growth.

The electrochemical results indicate the presence of a high stability oxide of both duplex stainless steels not only at the base metal but also at the stir zone of the FSWed samples. All Bode phase diagrams presented two peaks associated to the oxide layer formed on the surface of stainless steels and the charge transfer.

The corrosion resistance of the UNS S32205 was improved and the lean duplex UNS S32101 was decreased after FSW. Nevertheless, the resistance of the lean duplex UNS S32101 FSWed was still similar or higher than the traditional austenitic stainless steels.

ACKNOWLEDGEMENTS

The authors acknowledge Aperam and Outokumpu for providing the DSS plates and Petrobras, CNPq and FAPESP for the financial support.

References

1. Y. Yang, B. Yan and J. Li, J. Wang, *Corrosion Sci* 53 (2011) 3756.
2. Y. S. Sato and H. Kokawa, *Scripta Material* 40 (1999) 659.
3. J.W. Elmer, T.A. Palmer and E.D. Specht, *Diffraction Metal Material Trans* 38A (2007) 464.
4. ASM HANDBOOK, Volume 6, ASM International, Materials Park, OH, 1993, 1299.
5. E.M. Westin, Microstructure and properties of welds in the lean duplex stainless steel LDX 2101, Thesis. Department of Materials Science and Engineering. Royal Institute of Technology, Stockholm, 65p.
6. T. Saeid, A. Abdollah-zadeh, H. Assadi and F. Malek Ghaini, *Material Sci Eng A* 496 (2008) 262.
7. T. F. Fontes, R. Magnabosco, M. Terada, A. F. Padilha and I. Costa, *Corrosion* 4 (2011) 045004.
8. S.H.C. Park, Y.S.Sato, H.Kokawa, K. Okamoto, S.Hirano and M. Inagaki, *Scripta Material* 51 (2004) 101.
9. C. Garcia, F. Martin, P. de Tiedra, Y. Blanco and M. Lopez, *Corrosion Sci*, 50 (2008) 1184.
10. T.F.A. Santos, R.R. Marinho, M.T.P. Paes and A.J. Ramirez, *Revista Escola Minas* 66 (2013) 187.
11. Y.S. Sato, T.W. Nelson, C.J. Sterling, R.J. Steel and C.O. Petterson, *Material Sci Eng A* 397 (2005) 376.
12. R.J. Steel, C.J. Sterling, Friction stir welding of 2205 duplex stainless steel and 3Cr12 Steels, in: 14th International Society of Offshore and Polar Engineering Conference 2004, ISOPE 2004, Toulon, France, Vol. 4, p. 1-6.

13. T.F.A. Santos, A.J. Ramirez, Correlating Microstructure and Performance of UNS S32750 and S32760 Superduplex Stainless Steels Friction Stir Welds, in: 21th International Society of Offshore and Polar Engineering Conference 2011, Maui, Hawaii, p. 534-540.

© 2014 The Authors. Published by ESG (www.electrochemsci.org). This article is an open access article distributed under the terms and conditions of the Creative Commons Attribution license (<http://creativecommons.org/licenses/by/4.0/>).